

New approaches to testing and evaluating the impact capability of coal seam with hard roof and/or floor in coal mines

Y.L. Tan^{1,2a}, X.S. Liu^{*1,2}, B. Shen^{1,3b}, J.G. Ning^{1,2c} and Q.H. Gu^{2d}

¹State Key Laboratory of Mining Disaster Prevention and Control Co-founded by Shandong Province and the Ministry of Science and Technology, Shandong University of Science and Technology, Qingdao, China

²College of Mining and Safety Engineering, Shandong University of Science and Technology, Qingdao 266590, China

³CSIRO Energy, QCAT, 1 Technology Court, Pullenvale, Qld 4069, Australia

(Received March 27, 2017, Revised July 20, 2017, Accepted August 24, 2017)

Abstract. Samples composed of coal and rock show different mechanical properties of the pure coal or rock mass. For the same coal seam with different surrounding rocks, the frequency and intensity of rock burst can be significantly different in. First, a method of measuring the strain variation of coal in the coal-rock combined sample was proposed. Second, laboratory tests have been conducted to investigate the influences of rock lithologies, combined forms and coal-rock height ratios on the deformation and failure characteristics of the coal section using this method. Third, a new bursting liability index named combined coal-rock impact energy speed index (CRIES) was proposed. This index considers not only the time effect of energy, but also the influence of surrounding rocks. At last, a new approach considering the influences of roof and/or floor was proposed to evaluate the impact capability of coal seam. Results show that the strength and elastic modulus of coal section increase significantly with the coal-rock height ratio decreasing. In addition, the values of bursting liability indexes of the same coal seam vary greatly when using the new approach. This study not only provides a new approach to measuring the strain of the coal section in coal-rock combined sample, but also improves the evaluation system for evaluating the impact capability of coal.

Keywords: rock burst; coal-rock combined sample; impact capability; hard rock; impact energy speed

1. Introduction

Rock burst is one of the major dynamic disasters during the coal mining process, which seriously threatens the mining safety and productivity (Dehghan *et al.* 2013, Zhao *et al.* 2017, Tan *et al.* 2017, Song *et al.* 2017, Guo *et al.* 2017). The bursting liability is an effective and widely used reference to evaluate the impact capability of coal seam and rock mass (Jiang *et al.* 2011, Kidybiński 1981, Li *et al.* 2016, Cai *et al.* 2016). Researchers have proposed many kinds of bursting liability indexes to assess the impact capability of coal, such as the elastic energy index, impact energy index, dynamic failure duration, brittleness index, etc. (Kidybiński *et al.* 1981, Cai *et al.* 2016, Wang *et al.* 2014). These indexes reflect the impact capability of coal seam in different aspects, including energy, deformation, rigidity and some other factors. The Chinese standard,

Classification and laboratory testing method on bursting potential of coal (GBT 25217.2-2010) (2010), suggested using the dynamic failure duration, elastic energy index, impact energy index and uniaxial compressive strength together to assess the impact capability of coal.

In recent years, with the increase of mining depth in China, some rock bursts occurred in the coal seam that was assessed to have no impact capability (Procházka *et al.* 2014, Ning *et al.* 2016). And the frequency and intensity of rock burst during mining the same coal seam varied significantly with the surrounding rocks (Feng *et al.* 2011, Zuo *et al.* 2013, Wang *et al.* 2016, Liu *et al.* 2016). Considering the fact that the occurrence of rock burst depends not only on the mechanical properties of coal seam but also on the surrounding rocks, Li *et al.* (2005) and Dou *et al.* (2006) proposed assessing the impact capability of coal on the basis of the mechanical properties of the coal-rock combined sample. Liu *et al.* (2004), Wang *et al.* (2014), Zhao *et al.* (2016) and Huang *et al.* (2013) studied the influences of coal-rock height ratio, rock lithology, dip angle and loading rate on the mechanical properties of combined sample. Zhao *et al.* (2015) established a compression-shear strength criterion of the coal-rock combined sample considering interface effect. Although these researches have taken the influences of surrounding rocks into consideration to evaluate the impact capability of coal, the classifications have not been determined. Moreover, the impact capability of coal is affected by both the releasable energy and failure time. It gets stronger when the releasable energy increases and/or the dynamic failure

*Corresponding author, Ph.D.
E-mail: xuesheng1134@163.com

^aProfessor
E-mail: yunliangtan@163.com

^bProfessor
E-mail: baotang.shen@csiro.au

^cAssociate Professor
E-mail: njglxh@126.com

^dPh.D. Student
E-mail: 1090047040@qq.com

duration decreases, and vice versa.

On the other hand, researchers have proposed some new indexes to evaluate the impact capability of coal seam. By tracking the peak and trough values of elastic strain energy intensity before and after brittle failure, Jiang *et al.* (2010) put forward an index named local energy release rate and Qiu *et al.* (2014) established a relative energy release index. Tajduš *et al.* (2014) amended the classic elastic energy index from the relation of post-damage work of elastic strain to pre-damage work. Considering the time effect of energy, Pan *et al.* (2010) proposed an impact energy speed index, Zhang *et al.* (2009) established a residual energy release rate, and Yang *et al.* (2015) put forward a unit time relative local energy release index. The above indexes have higher accuracy and reliability than the previous indexes, especially the three indexes considering the effects of both energy and time. However, the indexes did not take the influences of surrounding rocks into consideration. The impact capability of coal seam might be underestimated because the loading effect of the hard roof and/or floor was ignored.

Bearing this in mind, this paper firstly proposed an approach to acquiring the strain variation of coal under coal-rock combined condition and then tested the mechanical properties of the coal section with different rock lithologies, combination forms and height ratios. Then, we established a new bursting liability index, namely combined coal-rock impact energy speed index (CRIES). In addition we proposed a new approach to evaluating the impact capability of coal seam with hard roof and/or floor. Finally, a case study in Daanshan Mine, Beijing Haohua Energy Resource Co., Ltd, China, was presented to demonstrate the procedure and validity of this approach.

2. Methodologies

2.1 Testing methodology

2.1.1 Approach to acquiring the strain variation of coal under combined condition

When the coal-rock combined sample is loaded by static pressure, the coal and rock sections have uniform stress as they are connected in series, but have unequal axial strain as they are different in mechanical properties. The testing devices cannot directly acquire the strain variations of the coal and rock sections (Panaghi *et al.* 2015, Yang 2015). Because the rigidity and strength of the coal are usually smaller than those of the rock mass, the deformation and failure features of coal section are quite different from those of the rock section during the loading process of the coal-rock combined sample. Zuo *et al.* (2011) and Zhao *et al.* (2008) conducted many experiments and found that the failure of combined sample was usually caused by the coal section breaking while the rock section maintained intact, as shown in Fig. 1. Due to the uneven strain distribution of coal section during the failure process, we cannot measure its strain variation directly.

As the rock section can maintain intact during the whole loading process, its strain is uniformly distributed. Therefore, we can obtain the strain variation of the rock section by gluing several strain gauges along its length on



Fig. 1 The typical failure conditions of coal-rock combined samples (Zuo *et al.* 2011, Zhao *et al.* 2008)

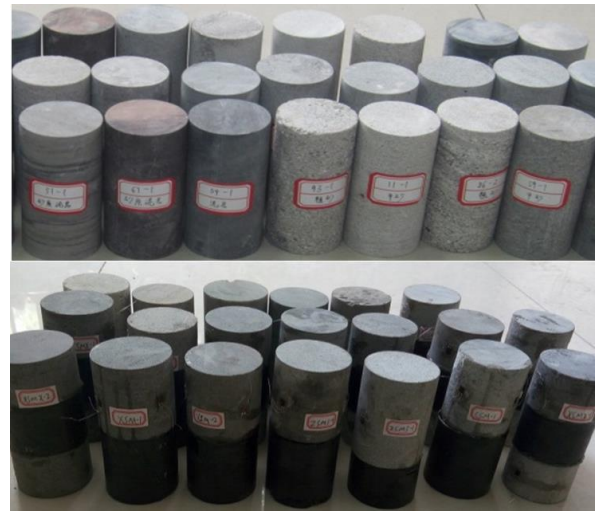


Fig. 2 Photos of some samples

Table 1 The sizes and some physical parameters of the samples

Sample nos.	Lithology	Rock-coal-rock heights /mm	Density /(kg/m^3)	P-wave velocity /(m/s)
XS-1,2,3	FS	100.03-0-0	2636.64	2198.4
ZS-1,2,3	MS	99.86-0-0	2455.45	2147.0
CS-1,2,3	CS	100.17-0-0	2254.33	1847.6
CM-1,2,3	Coal	0-99.72-0	1328.85	803.5
ZSM1-1,2,3	MS-Coal	50.06-50.11-0	1891.31	1526.5
CSM-1,2,3	CS-Coal	49.89-50.08-0	1793.68	1386.5
XSM-1,2,3	FS-Coal	50.12-50.03-0	1984.92	1593.7
ZSM2-1,2,3	MS-Coal	33.25-66.73-0	1612.51	1155.6
ZSM3-1,2,3	MS-Coal	66.67-33.29-0	2170.14	1842.4
XSMX-1,2,3	FS-Coal-FS	33.06-32.97-33.07	2205.58	1702.7
XSMZ-1,2,3	FS-Coal-MS	32.94-32.95-33.02	2140.35	1655.0
XSMC-1,2,3	FS-Coal-CS	33.11-33.06-32.95	2072.60	1593.6
ZSMZ-1,2,3	MS-Coal-MS	32.94-32.95-33.02	2079.03	1611.9
CSMC-1,2,3	CS-Coal-CS	33.11-33.06-32.95	1945.61	1469.5

Notes: FS, MS and CS are fine sandstone, medium sandstone and coarse sandstone, respectively. The second column is the lithology combination of each type of sample, the third column is the value of the No. 1 sample of each type, and the right two columns are the average values of each type of sample

its surface, and the influence of micro defects can be

eliminated by averaging the strain values at different locations. Combined with the deformation of combined sample, the strain of coal section can be obtained as

$$\varepsilon_C = \frac{\Delta h - \sum \varepsilon_{Ri} h_{Ri}}{h_C} \quad (1)$$

where ε_C and h_C are the strain and initial height of the coal section, respectively; Δh is the deformation amount of the combined sample; ε_{Ri} and h_{Ri} are the strain and initial height of the No. i rock section, respectively.

2.1.2 Samples preparation

There were one kind of coal sample and three kinds of rock samples. The coal, medium sandstone and coarse sandstone samples were respectively taken from No. 3 coal seam, its roof and floor in Xinhe Mine, Shandong Province, China. The fine sandstone samples were taken from the roof above No. 3-5 coal seam in Tongxin Mine, Shanxi Province, China. The samples were drilled and cut into cylinders with a diameter of 50 mm and a height of 25-100 mm, and the ends were grinded to ensure their smoothness with roughness less than 0.01 mm. One coal sample and one or two rock samples were glued together using epoxy resin adhesive to make a 100 mm high coal-rock combined sample, as shown in Fig. 2. Three high precision strain gauges were lengthwise glued on the surface of each rock section of the combined samples. There were 14 types of coal, rock and combined samples in total, and each type had three samples. The sizes and some basic physical parameters of the samples are shown in Table 1.

2.1.3 Testing devices and scheme

The AG-X250 Shimadzu Precision Universal Tester was used as the loading system. It is driven by motor servo, and the maximum load is 250 kN with the loading speed ranging from 0.0005 to 500 mm/min. The acoustic emission (AE) signals generated in the loading process were collected using the PCI-2 AE detector. The detector contains an 18-bit A/D converter, 4 high passes and 6 low passes, and its frequency ranges from 1 KHz to 3 MHz. It has good monitoring effect under complex noise, and can perform feature parameters extracting and waveform processing at the same time. The strain variations were collected by using the DH3815N static strain testing system.

Uniaxial loading tests of the samples listed in Table 1 were conducted using the AG-X250 Shimadzu Tester, and the displacement-controlled mode was applied with the loading rate of 0.001 mm/s. For the pure coal and rock samples, we used four sensors to monitor the AE signals during the loading process (Gholizadeh *et al.* 2015, Tan *et al.* 2016). The sensors were fixed with adhesive tape on the sample surface, with some Vaseline smearing on the interfaces, as shown in Fig. 3. The AE detector should run simultaneously with the loading system. The main parameters of the detector were set to be: main amplifier gain 40 dB, threshold 30 dB, floating threshold 5 dB, and resonance frequency 20-400 KHz. For the coal-rock combined samples, the strain gauges were in turn connected to the data-collecting box, the power controller and the control and data collecting center, as shown in Fig. 4. The

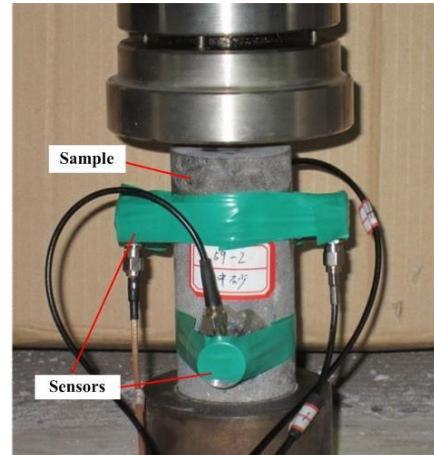


Fig. 3 Layout of the AE sensors



Fig. 4 Testing system of the coal-rock combined sample

system ran simultaneously with the loading system to monitor and record the value variations of strain gauges.

2.2 Assessment methodology

2.2.1 CRIES

Because of the differences in rigidity and micro structure, the rock and coal showed great differences in strength and deformation properties. During the loading process of coal-rock combined sample, the elastic strain energy accumulated in the rock section increases first and releases when the combined sample fails. The released energy will aggravate the failure of the coal section. The larger the elastic strain energy accumulated in the rock and coal sections, the more severe the coal failure, and the higher the impact capability of coal. Under the coal-rock combined condition, there may be a large amount of coal fragments flaked and ejected away, accompanied by some loud sounds, which are very similar to the impact failure characteristics of in-situ coal under hard roof.

Therefore, we proposed a new bursting liability index, CRIES. The new index took into consideration the time effect of released energy during the failure process, the mechanical properties of coal and surrounding rocks, and some other factors. The determination procedure is as follows:

Step 1. According to the height (H_1) of coal seam to be measured, the hard roof height (H_2) and the hard floor

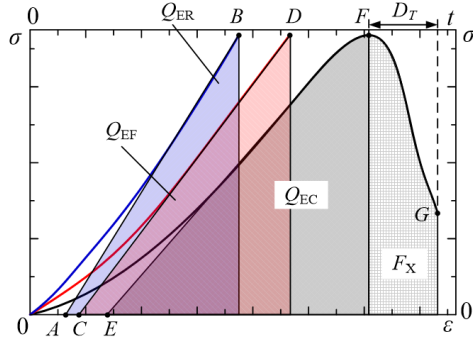


Fig. 5 The schematic diagram of loading results of the coal-rock combined sample (Q_{ER} is the area under line AB , Q_{EF} is the area under line CD , Q_{EC} is the area under curve EF , and F_X is the area under curve FG)

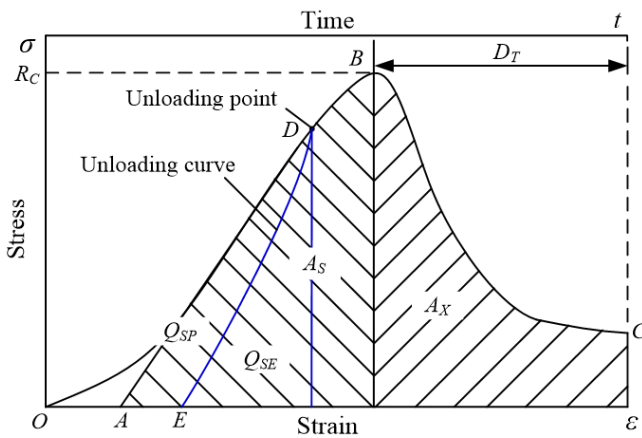


Fig. 6 The stress-strain curves of the coal section under one cyclic unloading and uniaxial loading (Q_{SP} is the area between curves OD and DE , Q_{SE} is the area under curve DE , A_S is the area under curve AB , A_X is the area under curve BC and D_T is the dynamic failure duration)

Table 2 Calculation and evaluation of the impact capability of coal seam

Index	Equation	Evaluation		
		No	Low	High
Elastic energy index	$W_{ET}=Q_{SE}/Q_{SP}$	$W_{ET}<2$	$2\leq W_{ET}<5$	$W_{ET}\geq 5$
Impact energy index	$K_E=A_S/A_X$	$K_E<1.5$	$1.5\leq K_E<5$	$K_E\geq 5$
Dynamic failure duration	D_T	$D_T>500$	$50<D_T\leq 500$	$D_T\leq 50$
Uniaxial compressive strength	R_C	$R_C<7$	$7\leq R_C<14$	$R_C\geq 14$
CRIES	Eq. (3)	$W_{ZT}<3$	$3\leq W_{ZT}<100$	$W_{ZT}\geq 100$

height (H_3), the heights of coal, roof rock and floor rock in the coal-rock combined sample can be respectively determined by Eq. (2). When the roof or floor is not harder than the coal, the height of the corresponding rock section in the combined sample should be zero.

$$h_1 = \frac{0.1H_1}{H_1 + H_2 + H_3}, \quad h_2 = \frac{0.1H_2}{H_1 + H_2 + H_3}, \quad h_3 = \frac{0.1H_3}{H_1 + H_2 + H_3} \quad (2)$$

where h_1 , h_2 and h_3 are the heights of coal, roof rock and floor rock in the coal-rock combined sample, respectively.

Step 2. By drilling, cutting and grinding, the coal, roof

rock and floor rock blocks taken from the underground were processed into samples with a diameter of 50 mm, and their heights are h_1 , h_2 and h_3 , respectively. The samples are glued together using epoxy resin adhesive in the sequence of roof-coal-floor into an integrated structure, which is the so called coal-rock combined sample.

Step 3. Glue the strain gauges on the lateral surface of the rock sections according to the approach demonstrated in Section 2.1.2, and load the combined samples axially. Then, we can draw the stress-strain curves of coal, roof rock and floor rock sections and the stress-time curve of the coal section, as shown in Fig. 5.

Step 4. According to Fig. 5, we can obtain the elastic energies accumulated in the roof rock, floor rock and coal sections, Q_{ER} , Q_{EF} and Q_{EC} , the dynamic failure duration, D_T , and the consumed energy of coal needed to break at the peak stress, F_X . Then, the value of CRIES, W_{ZT} , can be calculated as follows

$$W_{ZT} = \frac{h_2 Q_{ER} + h_3 Q_{EF} + h_1 Q_{EC}}{h_1 F_X \cdot D_T} \quad (3)$$

The impact energy speed index proposed by Pan *et al.* (2010) is the ratio of impact energy of a coal sample to its dynamic failure duration. According to the definitions of these two indexes, a coal sample and a coal-rock combined sample have the same impact capability when the value of impact energy speed index of the coal sample is equal to that of CRIES of the combined sample. Therefore, the evaluating criteria of the CRIES can be primarily determined as those of impact energy speed index, which are: $W_{ZT}<3$, no impact capability; $3\leq W_{ZT}<100$, low impact capability; $W_{ZT}\geq 100$, high impact capability.

2.2.2 Approach to evaluating the impact capability of coal seam with hard roof and/or floor

Considering the differences in the mechanical properties of coal seam with different rock lithologies and heights, we proposed evaluating the impact capability of coal seam by using the mechanical properties of coal and rock sections in the coal-rock combined sample instead of those of the pure coal sample. The evaluating procedure is as follows:

Step 1. Preparing the coal-rock combined samples, loading them in axial compression, and calculating the parameters, Q_{ER} , Q_{EF} , Q_{EC} , D_T and F_X , according to the Steps 1-4 in Section 2.2.1.

Step 2. Conducting one cyclic unloading test of the combined sample, and the unloading stress should be 75-85% of its uniaxial compressive strength. Then, we can obtain the elastic strain energy (Q_{SE}) and plastic strain energy (Q_{SP}) accumulated in the coal section at the unloading stress, as shown in Fig. 6. Conducting uniaxial loading test of the combined sample, and then the accumulated energy at peak stress (A_S) and the consumed energy after peak stress (A_X) of the coal section can be obtained (Fig. 6). Calculating the elastic energy index, impact energy index, dynamic failure duration, and uniaxial compressive strength based on the above parameters, and separately evaluating the impact capability of coal based on these indexes, as shown in Table 2 (GB/T 25217.2-2010, 2010).

Step 3. Calculating the value of the CRIES and

Table 3 Brief descriptions of No. 13 coal seam and its surrounding rocks in Daanshan Mine

Sequence	Rock name	Lithology	Thickness /m	Description
1	Main roof	Fine sandstone	5.62	Grey - black grey, medium - fine grained structure, muddy cementation.
2	Immediate roof	Siltstone	3.55	Grey black, compact, medium- and thick-bedded, silicon cementation.
3	No. 13 coal seam	Coal	2.50	Medium hard, mainly banded and granular structure.
4	Immediate floor	Siltstone	1.38	Grey black, compact, medium- and thick-bedded, silicon cementation.
5	Main floor	Medium sandstone	3.91	Black - grey, containing some Fe ₂ S concretions.

evaluating the impact capability of coal accordingly. Combined with the four indexes in Step 2, when the evaluation results of two or more indexes are “high”, the coal has high impact capability. When the evaluation results of all indexes are “no”, the coal has no impact capability. Otherwise, the coal has low impact capability.

2.2.3 Case description and samples preparation

A case study was conducted in the Daanshan Mine, Beijing Haohua Energy Resource Co., Ltd, China. It was located in the western mountains of Beijing. The No. 13 coal seam at +550 m level had simple structure with the average thickness of 2.5 m. Its roof and floor strata were hard and compact, and they were mainly siltstone, followed by fine sandstone and medium sandstone, as demonstrated in Table 3.

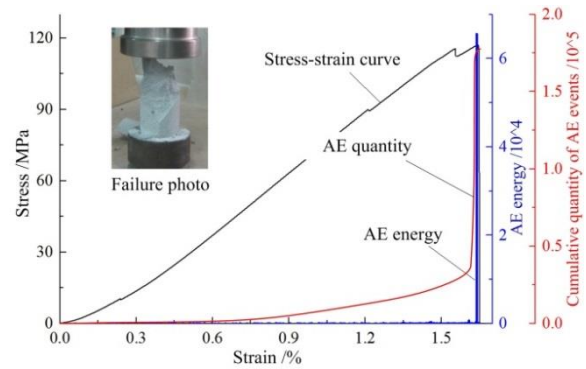
To obtain the mechanical properties of the coal seam with and without hard rocks, we took the No. 13 coal, its roof and floor samples in Daanshan Mine, and prepared the pure coal samples and the coal-rock combined samples with 50 mm in diameter and 100 mm in height. According to Eq. (2), the heights of coal, roof and floor sections in the combined samples were 33.65 mm, 47.78 mm and 18.57 mm, respectively. And the strain gauges were glued on the combined samples according to Section 2.1.2. The uniaxial loading test and one cyclic unloading test of the coal-rock combined samples were conducted according to Section 2.2.2, and these tests of the pure coal samples were conducted as comparison.

3. Results and discussion

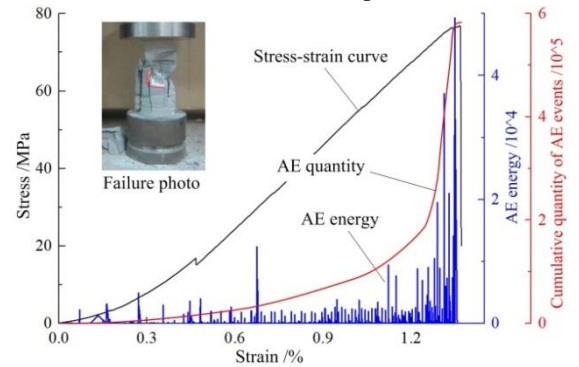
3.1 Testing results

3.1.1 The failure and AE features of coal and rock samples

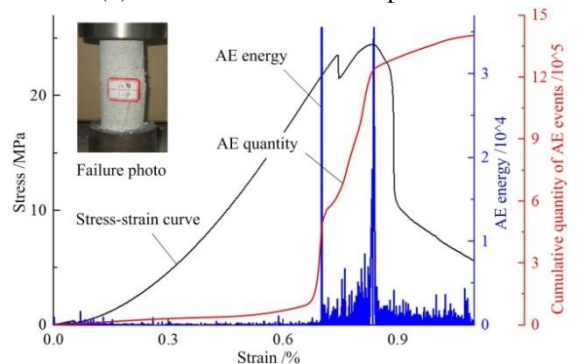
The stress-stain curves and variations of AE signals of the fine sandstone, medium sandstone, coarse sandstone and coal in Table 1 are shown in Fig. 7. As shown in the figure, the fine sandstone had no obvious compaction phase, with the peak stress of 116 MPa and peak strain of 0.0171. The compaction phase of medium sandstone was obvious, and its peak stress and strain were 77 MPa and 0.0138,



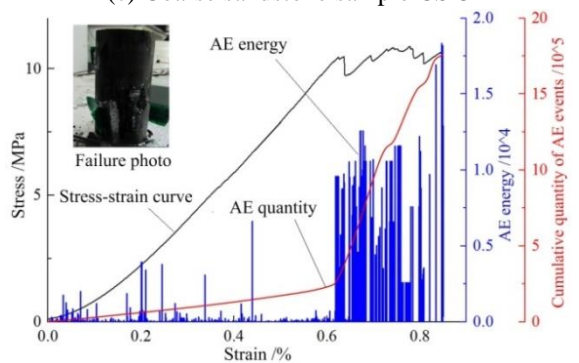
(a) Fine sandstone sample XS-2



(b) Medium sandstone sample ZS-1



(c) Coarse sandstone sample CS-3



(d) Coal sample CM-2

Fig. 7 The stress-strain curves and AE features of pure rock and coal samples

respectively. Both the two types of rocks had no obvious yield phase and the stress-strain curves dropped sharply after the peak stress, which meant that they experience typical brittle failure. The two types of rocks collapsed suddenly after the peak stress with loud sound and

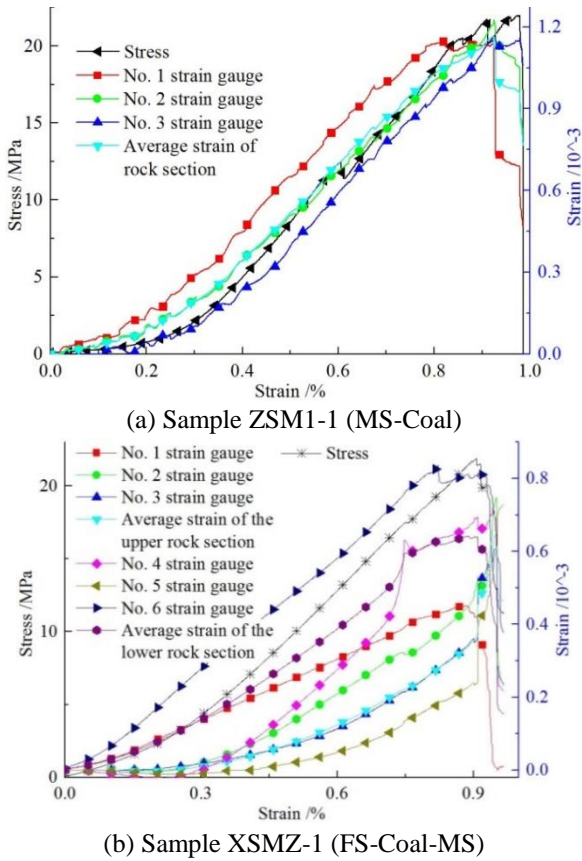


Fig. 8 Stress-strain curves of two combined samples and strain variations of their rock sections

vibrations, resulting in loss of the bearing capacity. The peak stress and strain of the coarse sandstone were 27.5 MPa and 0.0082, respectively, and it had obvious compaction and yield phases. The peak stress and strain of the coal sample were 11.5 MPa and 0.0078, respectively, with obvious compaction and yield phases too.

Before the peak stress of the fine sandstone, there were little AE events and the AE energy was very small. The quantity and energy of AE events increased significantly at the peak stress with the cumulative quantity of AE events of $1.74e5$ and the largest AE energy of $6.25e4$. In the compaction and elastic phases of the medium sandstone, there were a few AE events existing, with the largest energy of $1.2e4$. The AE events and energy increased significantly near the peak stress, and the largest energy and cumulative quantity of AE events were $4.9e4$ and $5.8e5$, respectively. Both the quantity and energy of AE events were small before the yield stress, and they increased sharply at the yield phase with the largest energy of $3.5e4$. After the peak stress, the bearing capacity decreased dramatically, and the cumulative quantity of AE events was $1.3e6$ with the energy decreased to $1e3-5e3$. The quantity and energy of AE events at the yield phase were high with the energy ranging from $2.5e3$ to $1.2e4$. The coal experienced brittle breaking after the yield phase with the largest energy of AE events being $1.75e4$ and the cumulative quantity being $1.7e6$.

During the loading process of these rocks, the sequence of the largest energy of AE events was fine sandstone>medium sandstone>coarse sandstone>coal, and that of the cumulative quantity was coal>coarse sandstone>medium

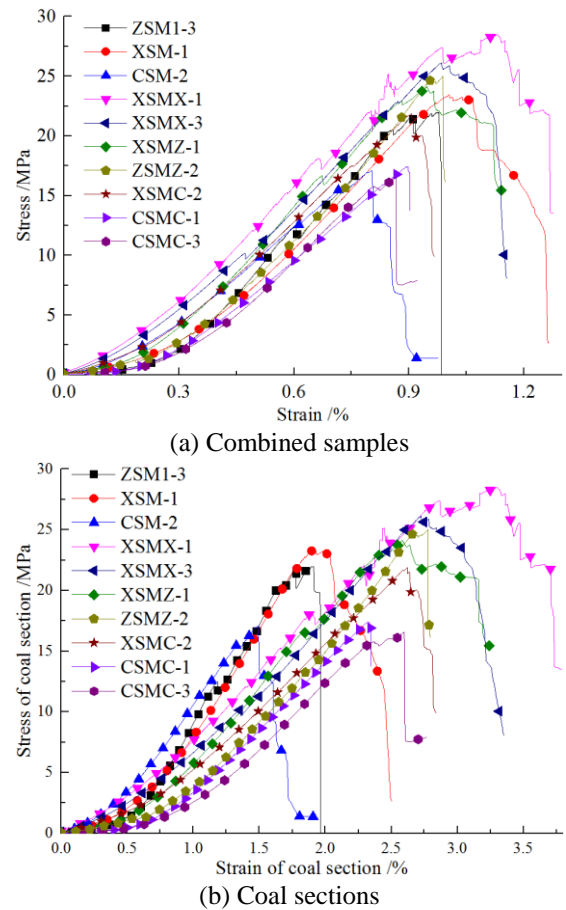


Fig. 9 Stress-strain curves of combined samples with different lithologies and combination forms (the lithology combinations of different sample numbers are listed in Table 1)



Fig. 10 Failure conditions of the combined samples

sandstone>fine sandstone. That was, the largest energy of AE events increased and the cumulative quantity decreased with the rock strength and brittleness increasing. The yield stresses of the three kinds of sandstones were larger than the uniaxial compressive strength of the coal, and the quantity and energy of AE events of the sandstones were small at the elastic phase, which meant that the sandstones deformed homogeneously before yielding. Therefore, we can use the approach demonstrated in section 2.1.1 to acquire the strain variations of coal in the combined samples with these

sandstones.

3.1.2 The influences of lithology on the mechanical properties of coal

During the loading process of the coal-rock combined samples, the stress and deformation variations of the combined samples can be obtained by the AG-X250 Shimadzu Tester, and the strain variations of the rock sections can be obtained from the DH3815N static strain testing system. Taking samples ZSM1-1 and XSMZ-1 as examples, the stress-strain curves of the combined samples and strain variations of their rock sections were shown in Fig. 8. The strain variations of coal sections can be calculated using Eq. (1), and the stress-strain curves of combined samples and coal sections were shown in Fig. 9. The failure conditions of the combined samples were shown in Fig. 10.

As shown in Fig. 8, the variation trend of rock section strain was similar to that of the combined sample stress, which meant that the rock section was in elastic state when the combined sample failed. As shown in Figs. 7(d), 9 and 10, the compressive strength and strain of the coal-rock combined sample were larger than those of the pure coal. The strengths and strains of the combined samples ranged respectively from 16.5 to 26 MPa and 0.0146 to 0.0326, 43.5-87.9 percent and 87.2-169.9 percent larger than those of the pure coal, respectively. When the height of rock was equal to that of coal in the two bodies combined sample, the strength and strain of coal section in the FS-Coal sample were larger than those of coal section in the MS-Coal sample, and those of coal section in the CS-Coal sample were the smallest. When the heights of the upper rock, coal and lower rock were equal in the three bodies combined sample, the strength and strain of coal section in the FS-Coal-FS sample were larger than those of coal section in the MS-Coal-MS sample, which were approximate to those of coal section in the CS-Coal-FS sample, followed by those of coal section in the MS-Coal-CS sample. The strength and strain of coal section in the CS-Coal-CS sample were the smallest.

In conclusion, when the heights of rock and coal sections were equal, the higher the rock strength, the higher the strength and strain of the coal section. For instance, the peak stress and strain of coal section in sample CSM-1 were respectively 16.3 MPa and 0.014, about 28.5% and 26.3% smaller than those of coal section in sample XSM-2, respectively. Moreover, the smaller the strength of the rock section in a combined sample, the more sharply the stress-strain curve dropped after the peak stress, and the smaller the fragment sizes. The reason may lie in the fact that the elastic energy accumulated in the rock sections increased with the rock rigidity decreasing and this energy will aggravate the failure of coal when the combined sample fails.

3.1.3 The influences of combination form on the mechanical properties of coal

As shown in Fig. 9, the combination form also had significant influence on the mechanical properties of coal section in the combined sample. The strength and strain of coal section in three bodies combined sample were higher

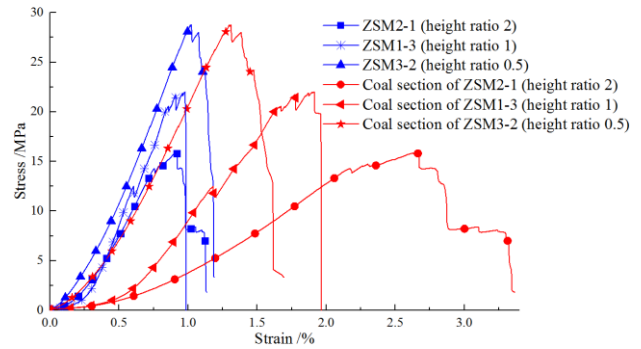


Fig. 11 Testing results of MS-Coal samples with different height ratios

and the Young's modulus was lower than those of coal section in two bodies combined sample even through the rock sections in combined samples were the same. For example, the strength, strain and Young's modulus of coal section in sample ZSM1-3 were respectively 21.5 MPa, 0.0183 and 1.58 GPa, while those of coal section in sample ZSMZ-2 were respectively 24.2 MPa, 0.028 and 1.24 GPa, the variations of which being 12.56%, 53% and -21.52%, respectively. Of course, the size difference of coal section may also contribute to the variations, which should be further studied.

3.1.4 The influences of coal-rock height ratios on the mechanical properties of coal

When the coal-rock height ratios of combined samples are different, the coal sections usually show different mechanical properties. Taking the MS-Coal samples as examples, the testing results were shown in Fig. 11.

As shown in the figure, when the coal-rock height ratio was 2.0, the strength of combined sample was 16.2 MPa, the peak strains of combined sample and coal section were respectively 0.009 and 0.0268, and the Young's modulus of coal section was 0.84 GPa. When the coal-rock height ratio reduced to 1.0, the strength of combined sample increased to 21.8 MPa, the peak strains of combined sample and coal section were respectively 0.0098 and 0.0189, and the Young's modulus of coal section increased to 1.77GPa, which represent a variation of 34.6%, 8.9%, -29.5% and 110.7%, respectively. When the coal-rock height ratio reduced to 0.5, the strength of combined sample increased to 28.7 MPa, the peak strains of combined sample and coal section were respectively 0.0104 and 0.013, and the Young's modulus of coal section increased to 2.86GPa, with the variations being 77.2%, 15.6%, -51.5% and 240.5%, respectively. Therefore, with the decreasing of the coal-rock height ratio, the strength and Young's modulus of coal section increased significantly, and the peak strain of coal section decreased.

3.2 Case analysis

The stress-strain curves of No. 13 coal seam, coal-rock combined samples, and coal and rock sections in Daanshan Mine are shown in Fig. 12. According to GB/T 25217.2-2010 (2010) and the approach demonstrated in Section 2.2.2, we evaluated the impact capability of No. 13 coal

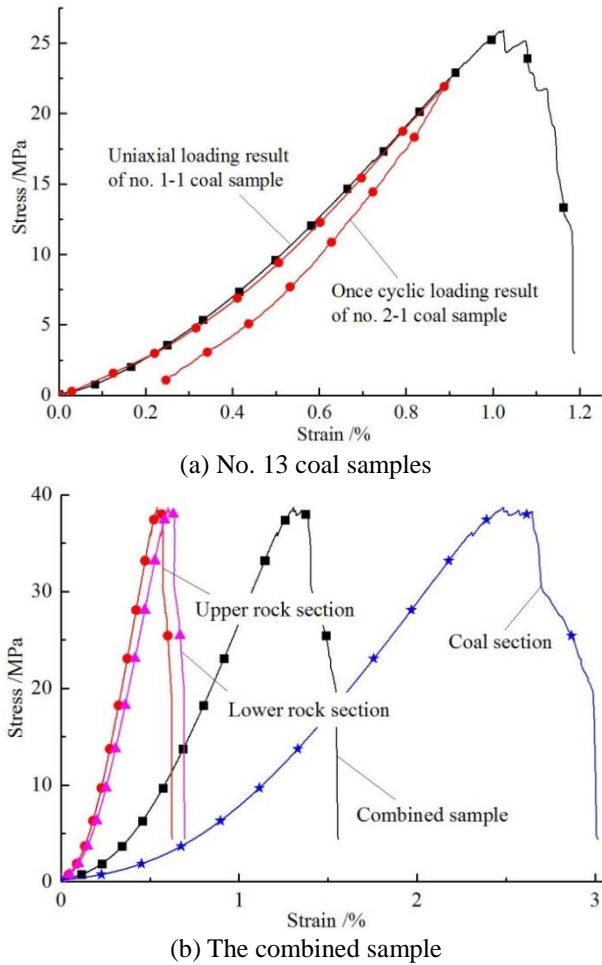


Fig. 12 Testing results of No. 13 coal and its combined sample in Daanshan Mine

Table 4 The impact capability of No. 13 coal seam at +550 m level in Daanshan Mine

Evaluation approaches	GB/T 25217.2-2010				Approach in Section 2.2.2				
Evaluation basis	Mechanical properties of the pure coal				Mechanical properties of coal and rock sections under combined condition				
Indexes	D_T /ms	W_{ET}	K_E	σ_C /MPa	D_T /ms	W_{ET}	K_E	σ_C /MPa	W_{ZT} /s ⁻¹
Values	139	3.82	3.57	25.31	87	4.35	5.29	38.56	112.8
Judgment	Low	Low	Low	High	Low	Low	High	High	High
Final results	Low impact capability				High impact capability				

Note: D_T -Dynamic failure duration; W_{ET} -Elastic energy index; K_E -Impact energy index; σ_C -Uniaxial compressive strength; W_{ST} -Impact energy speed index; W_{ZT} -CRIES

seam on the basis of the mechanical properties of the pure coal and the combined sample, respectively, and the results are shown in Table 4.

As shown in the table, when the mechanical properties of the pure coal were used as the evaluation basis, the values of the dynamic failure duration, elastic energy index, impact energy index and uniaxial compressive strength were 139 ms, 3.82, 3.57 and 25.31 MPa, respectively. Three of them were assessed to be “low” and one was assessed to be “high”, so the impact capability of No. 13 coal seam was finally assessed to be “low”. When evaluating the impact

capability of coal using the mechanical properties of the coal and rock sections under combined condition, the values of these four indexes were 87 ms, 4.35, 5.29 and 38.56 MPa, respectively. The value of the dynamic failure duration decreased by 37.4%, and the values of the elastic energy index, impact energy index and uniaxial compressive strength increased by 13.9%, 48.2% and 52.4%, respectively. And the value of the CRIES was 112.8/s. Compared with the evaluating criteria, the assessment results of the dynamic failure duration and elastic energy index were “low”, and the assessment results of the impact energy index, uniaxial compressive strength and CRIES were “high”. Therefore, No. 13 coal seam at +550 m level had high impact capability.

During the mining process of No. 13 coal seam at +550 m level in Daanshan Mine, there were several rock bursts occurring, which verified the coal seam having high impact capability. For example, two bursts occurred in the third east coal face and three bursts occurred in the second west coal face (Liu *et al.* 2016). Therefore, the proposed approach evaluating the impact capability of coal has effectively taken the influences of hard roof and/or floor into consideration and the evaluation results are in good agreement with the filed observation.

3.3 Discussion

(1) In underground engineering such as coal mining and tunnelling, the rocks with different lithologies usually bear the loads together, and the combined rock entity shows different mechanical properties with any one single rock. Taking the coal-rock combined sample as an example, the strength and Young’s modulus of the combined sample are higher and the failure is more violent than those of the pure coal sample. The coal-rock height ratio, lithology and dip angle all have strong influences on the mechanical properties of the combined sample (Zuo *et al.* 2011, 2013, Huang *et al.* 2013, Zhao *et al.* 2008, 2014, 2016). However, previous researches mainly focused on the mechanical properties of the combined samples, and those of one single section and their influence factors were rarely studied. In this paper, we proposed to back-calculating the strain variation of coal section under combined condition by measuring the strain variations of rock section from the strain gages glued on the rock surface. Experiments showed that this approach can accurately and effectively acquire the deformation and failure properties of coal section under combined condition. And the mechanical properties of coal sections with different rock lithologies, combination forms and coal-rock height ratios were obtained, which can provide more accurate evaluation of the impact capability of coal.

(2) The bursting liability index is an important parameter for assessing the impact capability of pure coal, and researchers have proposed many bursting liability indexes, such as the elastic energy index, impact energy index, dynamic failure duration, brittleness index, etc. Accurate assessment of the impact capability of coal plays a fundamental role in predicting and controlling the rock burst (Kidybiński 1981, Jiang *et al.* 2011, Cai *et al.* 2016). However, whether the occurrence of rock burst not only depends on the mechanical properties of coal, but also

depends on the lithology, structure and pressure of surrounding rocks (Procházka *et al.* 2014, Ning *et al.* 2016, Feng *et al.* 2011, Zuo *et al.* 2013, Wang *et al.* 2016, Hu *et al.* 2017, Ghanbari *et al.* 2014). Both the energy and time influence the impact capability of coal seam. Therefore, we established a new bursting liability index, namely CRIES, and proposed a new approach to evaluating the impact capability of coal seam with hard roof and/or floor. The CRIES took the time effect of energy during the failure process, the lithologies and heights of surrounding rocks and some other factors into consideration. And the new approach used the mechanical properties of coal and rock sections under combined condition as the evaluation basis and used the dynamic failure duration, elastic energy index, impact energy index, uniaxial compressive strength and CRIES as the evaluation indexes. Case analysis shows that the CRIES and the new approach can accurately evaluate the impact capability of coal seam with hard roof and/or floor, and they are in good agreement with the filed observations.

4. Conclusions

The aim of this research was to improve the evaluation accuracy of the impact capability of coal seam with hard roof and/or floor in coal mines. By comparing with the previous studies, this work contains at least three new aspects: (1) The mechanical properties of coal section in coal-rock combined sample with different rock lithologies, combination forms and height ratios were firstly obtained, by proposing an approach to acquiring the strain variations of coal section under combined condition. (2) A new bursting liability index (CRIES) considering the time effect of energy and the lithologies and heights of surrounding rocks was established. (3) A new approach using the mechanical properties of coal and rock sections under combined condition as the evaluation basis was proposed to evaluating the impact capability of coal seam with hard roof and/or floor.

Loading tests show that the AE quantity and energy of the coal and rock samples were small and the strains varied homogeneously before the yield stress. The mechanical properties of coal section in coal-rock combined sample can be effectively obtained by using the proposed method. The strength and peak strain of coal section under combined condition were higher than those of the pure coal, and they decreased with the decrease of strength of rock section. The strength and Young's modulus of coal section increased significantly and the peak strain decreased with the decrease of coal-rock height ratio.

When the mechanical properties of coal and rock sections under combined condition were used as the evaluation basis, the values of elastic energy index, impact energy index and uniaxial compressive strength increased while the value of dynamic failure duration decreased, which means that the assessed impact capability of coal increased. The impact capability of No. 13 coal seam at +550 m level in Daanshan Mine was assessed to be "high", which was in good agreement with the filed observation.

Of course, the approach to measuring the strain variation of coal section is restricted to the condition that the yield

stress of rock section is much higher than the strength of coal section. Moreover, it is necessary to conduct more case studies with different geological conditions to verify and improve the new evaluating approach.

Acknowledgments

This study was supported by National Natural Science Foundation of China (Nos. 51474137, 51574154 and 11602130), Doctoral Scientific Fund Project of the Ministry of Education of China (No. 20123718110013), Shandong Province Science and Technology Development Plan Item (2014GSF120002), Tai'shan Scholar Engineering Construction Fund of Shandong Province of China, and Scientific Research Foundation of Shandong University of Science and Technology for Recruited Talents.

References

- Cai, W., Dou, L.M., Si, G.Y., Cao, A.Y., He, J. and Liu, S. (2016), "A principal component analysis/fuzzy comprehensive evaluation model for coal burst liability assessment", *J. Rock Mech. Min. Sci.*, **81**, 62-69.
- Dehghan, S., Shahriar, K., Maarefvand, P. and Goshtasbi, K. (2013), "3-D modeling of rock burst in pillar No. 19 of Fetr6 chromite mine", *J. Min. Sci. Technol.*, **23**(2), 231-236.
- Dou, L.M., Lu, C.P., Mu, Z.L., Zhang, X.T. and Li, Z.H. (2006), "Rock burst tendency of coal-rock combinations sample", *J. Min. Safe. Eng.*, **23**(1), 43-46.
- Feng, X.J., Wang, E.Y., Shen, R.X., Wei, M.Y., Chen, Y. and Cao, X.Q. (2011), "The dynamic impact of rock burst induced by the fracture of the thick and hard key stratum", *Proc. Eng.*, **26**, 457-465.
- GB/T 25217.2-2010 (2010), *Methods for Test, Monitoring and Prevention of Rock Burst-Part 2: Classification and laboratory Test Method on Bursting Liability of Coal*, Standards Press of China, Beijing, China.
- Ghanbari, E. and Hamidi, A. (2014), "Numerical modeling of rapid impact compaction in loose sands", *Geomech. Eng.*, **6**(5), 487-502.
- Gholizadeh, S., Leman, Z. and Baharudin, B.T.H.T. (2015) "A review of the application of acoustic emission technique in engineering", *Struct. Eng. Mech.*, **54**(6), 1075-1095.
- Guo, W.Y., Zhao, T.B., Tan, Y.L., Yu, F.H., Hu, S.C. and Yang, F.Q. (2017), "Progressive mitigation method of rock bursts under complicated geological conditions", *J. Rock Mech. Min. Sci.*, **96**, 11-22.
- Hu, S.C., Tan, Y.L., Zhou, H., Guo, W.Y., Hu, D.W., Meng, F.Z. and Liu, Z.G. (2017), "Impact of bedding planes on mechanical properties of sandstone", *Rock Mech. Rock Eng.*, **50**(8), 2243-2251.
- Huang, B.X. and Liu, J.W. (2013), "The effect of loading rate on the behavior of samples composed of coal and rock", *J. Rock Mech. Min. Sci.*, **61**, 23-30.
- Jiang, Q., Feng, X.T., Xiang, T.B. and Su, G.S. (2010), "Rockburst characteristics and numerical simulation based on a new energy index: a case study of a tunnel at 2,500 m depth", *Bull. Eng. Geol. Environ.*, **69**(3), 381-388.
- Jiang, Y.D., Wang, H.W., Zhao, Y.X., Zhu, J. and Pang, X.F. (2011), "The influence of roadway backfill on bursting liability and strength of coal pillar by numerical investigation", *Proc. Eng.*, **26**, 1125-1143.
- Kidybiński, A. (1981), "Bursting liability indexes of coal", *J. Rock*

- Mech. Min. Sci. Geomech. Abstr.*, **18**(4), 295-304.
- Li, H.T., Zhou, H.W., Jiang, Y.D. and Wang, H.W. (2016), "An evaluation method for the bursting characteristics of coal under the effect of loading rate", *Rock Mech. Rock Eng.*, **49**(8), 3281-3291.
- Li, J.Q., Qi, Q.X., Mao, D.B. and Wang, Y.X. (2005), "Discussion on evaluation method of bursting liability with composite model of coal and rock", *Chin. J. Rock Mech. Eng.*, **24**(S1), 4805-4810.
- Liu, B., Yang, R.S., Guo, D.M. and Zhang, D.Z. (2004), "Burst-prone experiments of coal-rock combination at -1100 m level in suncun coal mine", *Chin. J. Rock Mech. Eng.*, **23**(14), 2402-2408.
- Liu, X.S., Ning, J.G., Tan, Y.L. and Gu, Q.H. (2016), "Damage constitutive model based on energy dissipation for intact rock subjected to cyclic loading", *J. Rock Mech. Min. Sci.*, **85**, 27-32.
- Liu, X.S., Tan, Y.L., Ning, J.G., Tian, C.L. and Tian, Z.W. (2016), "Energy criterion of abutment pressure induced strain-mode rockburst", *Rock Soil Mech.*, **37**(10), 2929-2936.
- Ning, J.G., Wang, J., Tan, Y.L. and Shi, X.S. (2016), "Dissipation of impact stress waves within the artificial blasting damage zone in the surrounding rocks of deep roadway", *Shock Vibr.*
- Pan, Y.S., Geng, L. and Li, Z.H. (2010), "Research on evaluation indexes for impact tendency and danger of coal seam", *J. Chin. Coal Soc.*, **35**(12), 1175-1178.
- Panaghi, K., Golshani, A. and Takemura, T. (2015), "Rock failure assessment based on crack density and anisotropy index variations during triaxial loading tests", *Geomech. Eng.*, **9**(6), 793-813.
- Procházka, P.P. (2014), "Rock bursts due to gas explosion in deep mines based on hexagonal and boundary elements", *Adv. Eng. Softw.*, **72**, 57-65.
- Qiu, S.L., Feng, X.T., Jiang, Q. and Zhang, C.Q. (2014), "A novel numerical index for estimating strainburst vulnerability in deep tunnels", *Chin. J. Rock Mech. Eng.*, **33**(10), 2007-2017.
- Song, D.Z., Wang, E.Y., Li, Z.H., Qiu, L.M. and Xu, Z.Y. (2017), "EMR: An effective method for monitoring and warning of rock burst hazard", *Geomech. Eng.*, **12**(1), 53-69.
- Tajduś, A., Cieślik, J. and Tajduś, K. (2014), "Rockburst hazard assessment in bedded rock mass: Laboratory tests of rock samples and numerical calculations", *Arch. Min. Sci.*, **59**(3), 591-608.
- Tan, Y.L., Guo, W.Y., Gu, Q.H., Zhao, T.B., Yu, F.H., Hu, S.C. and Yin, Y.C. (2016), "Research on the rockburst tendency and AE characteristics of inhomogeneous coal-rock combination bodies", *Shock Vibr.*, 1-11.
- Tan, Y.L., Liu, X.S., Ning, J.G. and Lu, Y.W. (2017), "In situ investigations on failure evolution of overlying strata induced by mining multiple coal seams", *Geotech. Test. J.*, **40**(2), 244-257.
- Wang, J.C., Jiang, F.X., Meng, X.J., Wang, X.Y., Zhu, S.T. and Feng, Y. (2016), "Mechanism of rock burst occurrence in specially thick coal seam with rock parting", *Rock Mech. Rock Eng.*, **49**(5), 1953-1965.
- Wang, T., Jiang, Y.D., Zhan, S.J. and Wang, C. (2014), "Frictional sliding tests on combined coal-rock samples", *J. Rock Mech. Geotech. Eng.*, **6**(3), 280-286.
- Yang, F.J., Zhou, H., Lu, J.J., Zhang, C.Q. and Hu, D.W. (2015), "An energy criterion in process of rockburst", *Chin. J. Rock Mech. Eng.*, **34**(S1), 2706-2714.
- Yang, S.Q. (2015), "An experimental study on fracture coalescence characteristics of brittle sandstone specimens combined various flaws", *Geomech. Eng.*, **8**(4), 541-557.
- Zhang, X.Y., Feng, G.R., Kang, L.X. and Yang, S.S. (2009), "Method to determine burst tendency of coal rock by residual energy emission speed", *J. Chin. Coal Soc.*, **34**(9), 1165-1168.
- Zhao, T.B., Guo, W.Y., Lu, C.P. and Zhao, G.M. (2016), "Failure characteristics of combined coal-rock with different interfacial angles", *Geomech. Eng.*, **11**(3), 345-359.
- Zhao, T.B., Guo, W.Y., Tan, Y.L., Lu, C.P. and Wang, C.W. (2017), "Case histories of rock bursts under complicated geological conditions", *Bull. Eng. Geol. Environ.*, 1-17.
- Zhao, Z.H., Wang, W.M., Wang, L.H. and Dai, C.Q. (2015), "Compression-shear strength criterion of coal-rock combination model considering interface effect", *Tunn. Undergr. Sp. Technol.*, **47**, 193-199.
- Zuo, J.P., Wang, Z.F., Zhou, H.W., Pei, J.L. and Liu, J.F. (2013), "Failure behavior of a rock-coal-rock combined body with a weak coal interlayer", *J. Min. Sci. Technol.*, **23**(6), 907-912.

CC